Virology 477 (2015) 110–118

Contents lists available at ScienceDirect

Virology

journal homepage: www.elsevier.com/locate/yviro

Receptor binding proteins of *Listeria monocytogenes* bacteriophages A118 and P35 recognize serovar-specific teichoic acids

Regula Bielmann [a,1], Matthias Habann [a,1], Marcel R. Eugster [a], Rudi Lurz [b], Richard Calendar [c], Jochen Klumpp [a,*], Martin J. Loessner [a]

[a] Institute of Food, Nutrition and Health, ETH Zurich, Schmelzbergstrasse 7, 8092 Zurich, Switzerland
[b] Max-Planck Institute for Molecular Genetics, 14195 Berlin, Germany
[c] Department of Molecular and Cell Biology, University of California, Berkeley, CA 94720-3202, USA

ARTICLE INFO

Article history:
Received 24 October 2014
Returned to author for revisions
19 December 2014
Accepted 22 December 2014
Available online 21 February 2015

Keywords:
Caudovirales
Phage adsorption
Baseplate model
Fluorescence microscopy
Immuno-gold labeling
Phage crosslink

ABSTRACT

Adsorption of a bacteriophage to the host requires recognition of a cell wall-associated receptor by a receptor binding protein (RBP). This recognition is specific, and high affinity binding is essential for efficient virus attachment. The molecular details of phage adsorption to the Gram-positive cell are poorly understood. We present the first description of receptor binding proteins and a tail tip structure for the siphovirus group infecting *Listeria monocytogenes*. The host-range determining factors in two phages, A118 and P35 specific for *L. monocytogenes* serovar 1/2 have been determined. Two proteins were identified as RBPs in phage A118. Rhamnose residues in wall teichoic acids represent the binding ligands for both proteins. In phage P35, protein gp16 could be identified as RBP and the role of both rhamnose and N-acetylglucosamine in phage adsorption was confirmed. Immunogold-labeling and transmission electron microscopy allowed the creation of a topological model of the A118 phage tail.

Introduction

Listeria monocytogenes is an opportunistic, Gram-positive, non spore-forming pathogen responsible for severe infections in both animals and humans and associated with a high mortality rate of up to 30% (Vazquez-Boland et al., 2001). The genus *Listeria* encompasses ten closely related species, now including the recently described new species *L. rocourtiae* (Leclercq et al., 2010), *L. marthii* (Graves et al., 2010), *L. weihenstephanensis* (Lang Halter et al., 2013) and *L. fleischmanni* (Bertsch et al., 2013). Primarily associated with human infections are *L. monocytogenes* strains of the serovars (SV) 1/2a, 1/2b and 4b (Farber and Peterkin, 1991). The SV 1/2 group is defined by two different sugar residues linked to the C2 and C4 positions of the linear ribitol-phosphate backbone of the wall teichoic acids (WTA), namely rhamnose and N-acetylglucosamine. In contrast, SV 4b cell walls has a WTA type featuring a complex secondary substitution of integrated N-acetylglucosamine with terminal glucose and galactose (Eugster and Loessner, 2012; Fiedler, 1988; Uchikawa et al., 1986).

Bacteriophages have emerged as versatile tools for detection and biocontrol of foodborne pathogens, such as *Listeria*. Phage based detection methods can be used to trace the source of bacterial contamination and outbreaks, and help to identify and characterize associated strains (Loessner and Busse, 1990). The application of reporter phages, allows for a rapid detection of viable *Listeria* cells in food and environmental samples (Loessner et al., 1996; Hagens et al., 2011). Phage products are also used to sanitize food products and production facilities from *Listeria* contaminations (Carlton et al., 2005). Altogether, a prerequisite for use of phages in biocontrol and detection is the understanding of molecular details of the adsorption and infection processes (Habann et al., 2014).

The first step in the infection of a bacterial host by a bacteriophage is the adsorption of the phage to the host cell. The attachment of the virus particle requires recognition of a cell wall associated ligand (commonly referred to as phage receptor) by a phage receptor binding protein (RBP). The RBP recognition and binding is extremely specific, and high affinity is required for rapid and efficient virus attachment. Most of our knowledge about this interaction originates from research on T-phages and lambdoid phages infecting *Escherichia coli* and related organisms (Chatterjee and Rothenberg, 2012; Killmann et al., 1995; Marti et al., 2013; Rossman and Yap, 2014). Apart from some intensive research on *Bacillus* phages and phages of lactic acid bacteria, little is known about the infection process for most phages infecting Gram-positive bacteria. Over the past decade or so, several RBP encoding genes of *Streptococcus thermophilus* phages DT1 and MD4, *Bacillus*

* Corresponding author. Tel.: +41 44 632 5378.
E-mail address: jochen.klumpp@hest.ethz.ch (J. Klumpp).
[1] Both authors contributed equally to this work.

http://dx.doi.org/10.1016/j.virol.2014.12.035
0042-6822/

subtilis phages SPP1 and φ29, *Lactococcus lactis* phages bIL67 and CHL92 of the c2 species, sk1, bIL170, and p2 of the 936 species, and TP901-1 and Tuc2009 belonging to the P335 species, have been identified (Bebeacua et al., 2013; De Haard et al., 2005; Duplessis and Moineau, 2001; Dupont et al., 2004; Guo et al., 2003; Jakutyte et al., 2012; Sciara et al., 2008; Spinelli et al., 2006a, 2014; Stuer-Lauridsen et al., 2003; Vegge et al., 2006). Most of these proteins likely bind to cell wall associated carbohydrates such as teichoic acids, as it has been proposed for *Bacillus* phage SPP1 (Baptista et al., 2008). For some RBPs, phosphoglycerol binding has been demonstrated (Ricagno et al., 2006; Sciara et al., 2010; Siponen et al., 2009). We have recently been able to determine molecular details and some structural information on the RBPs of the large virulent *Listeria* myovirus A511 (Habann et al., 2014). However, no data have been available for the numerous siphoviruses of pathogenic Gram-positive bacteria in general, and specifically for *Listeria*.

Listeria phage A118 has been isolated from a *L. monocytogenes* SV 1/2 lysogen (Loessner, 1991). It features a non-contractile tail of 300 nm in length, an isometric capsid with diameter of 61 nm (Dorscht et al., 2009a; Zink and Loessner, 1992), and belongs to the *Siphoviridae* family of dsDNA bacterial viruses in the order *Caudovirales*. Phage A118 represents the prototype of the temperate *Listeria* phages, and was the first to be sequenced and analyzed in some molecular detail (Loessner et al., 2000). Its 40.8 kb genome encodes 72 gene products, and is organized in three life-cycle specific gene clusters.

Listeria phage P35 shares no homology to A118 or other known *Listeria* phages except for P40, and belongs to a recently described class of virulent *Listeria Siphoviridae* featuring an approximately 57 nm head diameter and a 110 nm tail (Dorscht et al., 2009b). Its genome is 35.8 kb in size and contains 56 putative ORFs. In contrast to A118, P35 can infect most *Listeria* SV 1/2 strains. It lacks lysogeny control genes and therefore features a virulent (i.e. obligate lytic) lifestyle (Dorscht et al., 2009b; #1247). We selected both phages for this study, since their different morphologies and genomes, but the ability to infect the same *Listeria* serovars, might reveal common elements in receptor recognition and adsorption to the host cell.

We here report the identification of the proteins of both phages A118 and P35 responsible for binding to the host cell receptor. The cellular receptors for the RBP proteins have been identified as sugar side-chains of the wall teichoic acids. Employing various approaches, a topological model of the bacteriophage A118 baseplate could be created. Our data provide insights into the early stages of phage infection and elucidate important steps in the process of cell recognition and adsorption by these viruses.

Results

A118 and P35 baseplate proteins feature homologies to known phage tail proteins

A *in silico* analysis was performed to identify putative functions to A118 and P35 baseplate proteins and RBP candidates. Genes located between *tmp*, encoding the tape measure protein Tmp (gp16 in A118 and gp14 in P35) (Katsura, 1987), and the holin/endolysin lysis cassette (Loessner et al., 1995), were considered putative baseplate proteins (Fig. 1).

HHpred analyses revealed strong structural homologies of A118 gp17 to the distal tail proteins (Dit) gp46 of *Lactococcus* phage TP901-1 and gp19.1 of *Bacillus* phage SPP1, both described as central core proteins involved in adsorption apparatus assembly (Veesler et al., 2010, 2012). Strong homologies to gp44, forming a central hub involved in DNA translocation in *Enterobacteria* phage Mu, could be detected for A118 gp18 (Kondou et al., 2005). A118 gp19 is homologous to several proteins involved in receptor recognition and cell infection (Barbirz et al., 2008; Muller et al., 2008). Homologies to baseplate proteins of *Lactococcus* phage TP901-1 could be identified for A118 gp20. The N-terminal part of A118 gp20 resembles TP901-1 gp48 (BppU), while the C-terminal part is homologous to another TP901-1 baseplate protein gp49 (BppL), which was previously described as RBP (Vegge et al., 2006). Additionally, the C-terminal region shares structural similarity to the RBP of *Lactococcus* phage p2 (Bebeacua et al., 2013). No significant hits to phage related proteins could be identified for A118 gp21, gp22 or gp23.

Gp15, gp16 and gp17 were considered as putative RBPs in phage P35, due to their location at the end of the structural genes, downstream of Tmp (gp14) (Fig. 1). Bioinformatics revealed homologies to gp19.1 (Dit) of *Bacillus* phage SPP1 in the N-terminal and C-terminal parts of P35 gp15, while a homology to gp15 (Dit) of *Lactococcus* phage p2 was restricted to 232 aa residues in the N-terminal part. The P35 gp16 protein features a C-terminal homology to a putative prophage tail protein (gp18) from *L. monocytogenes* EGDe, and P35 gp17 exhibits a homology to the *Lactococcus* phage p2 receptor binding protein. No homologies could be found among the amino acid sequence of the putative RBPs in phage A118 (gp19 and gp20), and the protein sequences of the RBP candidates of P35, despite the fact that both phages infect SV 1/2 strains of *Listeria*. Interestingly, the N-termini of A118 gp19 and gp20 feature strong homology to the N-terminal part of the gp19 and gp20 of *Listeria* phage A500, which infects *Listeria* SV 4b strains (Dorscht et al., 2009b; Loessner and Busse, 1990; Zink and Loessner, 1992), while the C-terminus is highly variable. Taken together, *in silico* analyses allowed us to assign putative functions to most A118 baseplate proteins. Gp19 and gp20 represent putative RBPs in A118, but are unrelated to the RBP candidates gp15, gp16 and gp17 in P35.

The RBPs of A118 and P35 recognize specific sugar residues in Listeria cell wall teichoic acids

We aimed to experimentally confirm the function of the RBPs of phages A118 and P35, i.e., binding to their corresponding host cell receptors. Towards this aim, N-terminal GFP-fusions of the proteins were tested for their ability to bind to *Listeria* cells. We found that both A118 GFP-gp19 and A118 GFP-gp20 were able to evenly coat *Listeria* SV 1/2 cells (Fig. 2A and B), but not the other *Listeria* serovars tested, suggesting that both proteins contribute to the host-specificity of A118. Regarding phage P35, only gp16 exhibited specific adsorption to SV 1/2 cells (Fig. 2C), and this protein was confirmed to be the RBP of phage P35.

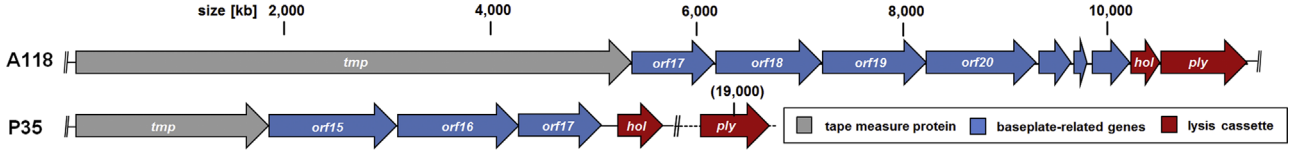

Fig. 1. Genomic localization of putative baseplate genes in bacteriophages A118 and P35. Genes located in between *tmp* (indicated in gray) and the holin/endolysin encoding genes (indicated in red) were considered as putative baseplate protein-encoding genes including RBP candidates (indicated in blue).

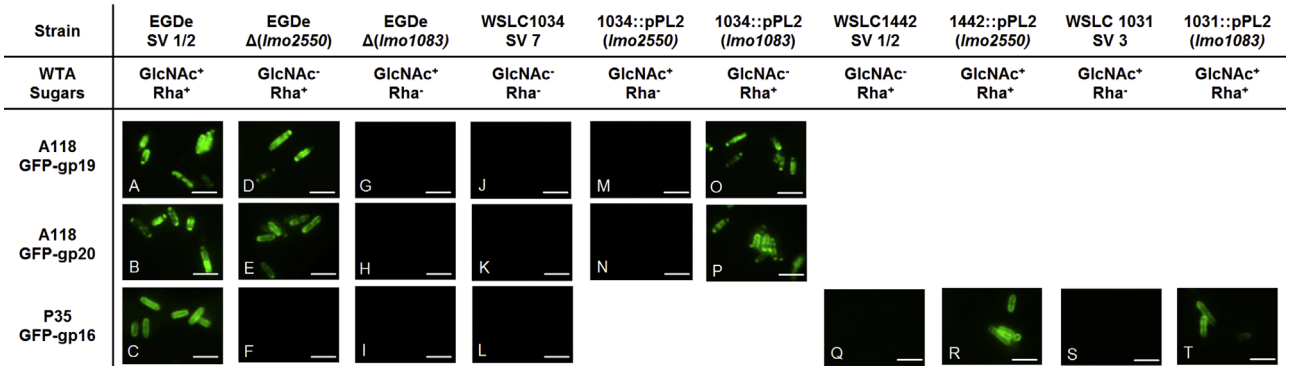

Fig. 2. Identification binding ligands (receptors) for *Listeria* phages A118 and P35. Confocal microscopy of *Listeria monocytogenes* cells incubated with purified A118 GFP-gp19, GFP-gp20, or P35 GFP-gp16. (Panels A–C): Binding to wildtype SV 1/2 strain EGDe. Binding to mutants deficient for N-acetylglucosamine (GlcNAc) in their wall teichoic acid can be detected for GFP-gp19 and GFP-gp20 (D and E), but not for GFP-gp16 (F). No binding could be observed to rhamnose (Rha) deficient mutants (G–I), and no binding occurs to the SV 7 strain (WSLC 1034) lacking both sugar substitutions (J–L). Restoring of N-acetylglucosamine substitution in the WTA polymer of WSLC 1034 did not enable binding of A118 GFP-gp19 and GFP-gp20 (M and N), whereas restoring rhamnose supported recognition by both proteins (O and P). WSLC1442 lacks GlcNAc and does not bind P35 GFP-gp16, whereas a GlcNAc-reconstituted strain does (Q and R). Serovar 3 cells feature only GlcNAc and no rhamnose, and do not allow binding (S) until rhamnose is introduced (T). Scale bars correspond to 5 μm.

Table 1
Binding properties of GFP-RBP fusion proteins, adsorption of phage particles to the bacterial cell wall, and infectivity of phages. +/− indicates a positive/negative result for GFP-RBP binding, adsorption of phage particles to *Listeria* spp. or host susceptibility to phage infection.

Species	Strain (WSLC)	Serovar	Binding of A118 GFP-gp19	Binding of A118 GFP-gp20	Adsorption of A118 to bacterial cell wall	A118 plaque formation	Binding of P35 GFP-gp16	Adsorption of P35 to bacterial cell wall	P35 plaque formation
L. monocytogenes	EGDe	1/2a	+	+	+	+	+	+	+
L. monocytogenes	Mack	1/2a	+	+	+	+	+	+	+
L. monocytogenes	1442	1/2a	+	+	+	+	−	−	−
L. monocytogenes	1066	1/2b	+	+	+	+	+	+	+
L. monocytogenes	1083	1/2b	+	+	+	−	+	+	+
L. monocytogenes	1001	1/2c	+	+	+	+	+	+	+
L. monocytogenes	1031	3b	−	−	−	−	−	−	−
L. monocytogenes	1032	3c	−	−	−	−	−	−	−
L. monocytogenes	1020	4a	−	−	−	−	−	−	−
L. monocytogenes	1042	4b	−	−	−	−	−	−	−
L. monocytogenes	1019	4c	−	−	−	−	−	−	−
L. monocytogenes	1033	4d	−	−	−	−	−	−	−
L. ivanovii	3009	5	−	−	−	−	−	−	−
L. ivanovii	3010	5	−	−	−	−	−	−	−
L. innocua	2021	6a	−	−	−	−	−	−	−
L. innocua	2054	6a	−	−	−	−	−	−	−
L. innocua	2653	6b	−	−	−	−	−	−	−
L. innocua	20105	6b	−	−	−	−	−	−	−
L. innocua	2024	6b	−	−	−	−	−	−	−
L. innocua	2012	6b	−	−	−	−	−	−	−
L. monocytogenes	1034	7	−	−	−	−	−	−	−

Both A118 and P35 can only infect SV 1/2 strains of *Listeria*. Characteristic sugar substituents, namely N-acetylglucosamine (GlcNAc) and rhamnose (Rha) in the WTA polymers are thought to serve as possible receptors for phage attachment, i.e., binding of the corresponding RBP (Eugster et al., 2011; Eugster and Loessner, 2012; Eugster et al., submitted for publication). Specific attachment to Rha residues has previously been demonstrated for phage A118 (Eugster and Loessner, 2012), and the requirement for both Rha and GlcNAc has been shown for the short tail fiber protein of *Listeria* phage A511 (Eugster et al., submitted for publication; Habann et al., 2014). Here, we assessed the function of RBP candidate proteins by adsorption tests with GFP-tagged RBP proteins (Fig. 2). Cell wall mutant strains lacking either GlcNAc (EGDeΔ*lmo2550*) or Rha (EGDeΔ*lmo1083*) in wall teichoic acids (Eugster et al., submitted for publication) were used in a first experiment (Fig. 2). GFP-gp19 and GFP-gp20 of A118 bound to EGDeΔ*lmo2550* (Fig. 2D and E) but not to EGDeΔ*lmo1083* (Fig. 2G and H), indicating a requirement for the presence of WTA rhamnose for binding of A118 gp19 and gp20 to the bacterial cell. Interestingly, the P35 RBP gp16 did not bind to either the ΔGlcNAc or the ΔRha mutant (Fig. 2F and I), suggesting that both sugar residues are required for cell wall recognition and phage adsorption. Neither A118 gp19 or gp20, nor P35 gp16 displayed binding to cells lacking both GlcNAc and Rha (Fig. 2J–L). Furthermore, no binding occurred to cells in which only GlcNAc (1034::pPL2(*lmo2550*)) in WTA was restored by complementation (Fig. 2M and N). However, reconstitution of rhamnose in 1034::pPL2(*lmo1083*) resulted in binding of both A118 RBP proteins (Fig. 2O and P), which demonstrated the requirement for this sugar in binding of A118 to its target cell.

Reconstitution of GlcNAc in WSLC 1442 (SV 1/2), restored the binding capability of P35 gp16 to wildtype levels (Fig. 2Q and R). Additional evidence that both sugars might be involved in receptor recognition resulted from assays using a SV 3 strain (WSLC 1031), which lacks rhamnose, and is unable to bind GFP-gp16 (Fig. 2S). When Rha was supplied by *trans* complementation (1031::pPL2 *(lmo1083)*), binding of gp16 could be observed (Fig. 2T).

The above results were matched with data obtained from pull down assays, which can quantify phage adsorption (Eugster et al., submitted for publication), and compared to host range spectra of both A118 and P35 (Table 1). A clear correlation between cell wall binding of both RBPs, adsorption of whole phage to its *Listeria*

target, and plaque formation (i.e., successful completion of lytic cycle by the phage) was found for A118, however, restricted to *Listeria* SV 1/2 hosts. One exception is strain WSLC 1083, which was decorated by GFP-gp19, GFP-gp20, and the A118 phage itself, but not yield plaques. Binding of P35 phage, P35 GFP-gp16, and infection range also matched perfectly, and were also limited to strains of SV 1/2 only (Table 1).

A118 gp18, gp19, and gp20 are required for attachment

Antibodies raised against putative tail components were employed to evaluate the role of the different A118 baseplate proteins in attachment and infection. The infectivity of phage particles after pre-incubation with sera containing the specific antibodies was investigated by quantitative phage plating. Pre-incubation of phage A118 particles with antibodies α-gp16, α-gp17, and α-gp21 had no effect on the phage infectivity (Fig. 3). In contrast, exposure to α-gp18, α-gp19, and α-gp20 completely inhibited phage infection, suggesting that the corresponding phage proteins gp18, gp19, and gp20 play essential roles in the early steps of phage infection (i.e., virus attachment), and are accessible to antibodies in the mature phage particle.

Topological model of the A118 tail tip

The major goal of this study was identification and localization of the individual A118 tail components, which would enable development of a structural model for the A118 baseplate. Towards these aims, antibodies against gp16 to gp21 were used in transmission electron microscopy (TEM) experiments. The antibodies were used to crosslink phage particles by their two antigen binding sites (Fig. 4A and B). A secondary, gold conjugated anti-rabbit antibody was employed to better visualize precise locations of the primary antibodies attached to the phage particles (Fig. 4C). Antibody α-gp16 (directed against the C-terminus of Tmp) bound at the interconnection of tail tube and tail tip. Interestingly, α-gp17 crosslinked the virus particles at two different positions within the phage baseplate: one located directly below gp16 at the interconnection of tail to tail tip, and the other in between the upper and lower baseplate "discs". These findings suggested that gp17 may form an inner core of the tail tip, and remains accessible from different sites. A118 α-gp18 was able to bind at the center of the lower baseplate ring, while binding of α-gp19 was restricted to the lower baseplate ring. Antibody α-gp20 crosslinked phages at the upper baseplate ring. Lastly, α-gp21 crosslinking demonstrated that the connection of upper and lower baseplate ring is at least partly made up of A118 gp21. Since each of the different antibodies bound in a characteristic pattern, we were able to allocate all of the tested putative baseplate proteins to distinct positions within the A118 baseplate structure. In conjunction with data obtained by TEM, a hypothetical model of the A118 tail tip could be generated (Fig. 5).

Discussion

The precise mechanism by which a phage particle recognizes, adsorbs to, and infects a bacterial cell is only poorly understood, especially for phages infecting Gram-positive pathogens. Most of our current knowledge on the early steps of infection stems from research on phages infecting Gram-negative bacteria, such as T4 (Leiman et al., 2010) and lambda (Wang et al., 2000; Werts et al., 1994). However, these data are of only limited value for the study of phages recognizing and attaching to Gram-positive cells. Research on the latter has mostly focused on model organisms from dairy-production environments and *Bacillus* phages (partially reviewed in Jakutyte et al., 2012; Spinelli et al., 2014), and almost no data are available on the adsorption process of phages of Gram-positive pathogens such as *Listeria* and *Staphylococcus* (Habann et al., 2014). In this work, we identified the receptor binding protein (RBP) and its corresponding binding ligands (receptors) in the two unrelated *Listeria* phages A118 and P35, which exclusively infect strains of SV 1/2. A118 and the smaller P35 do not only differ in terms of lifestyle (temperate vs. virulent), and lack of recognizable

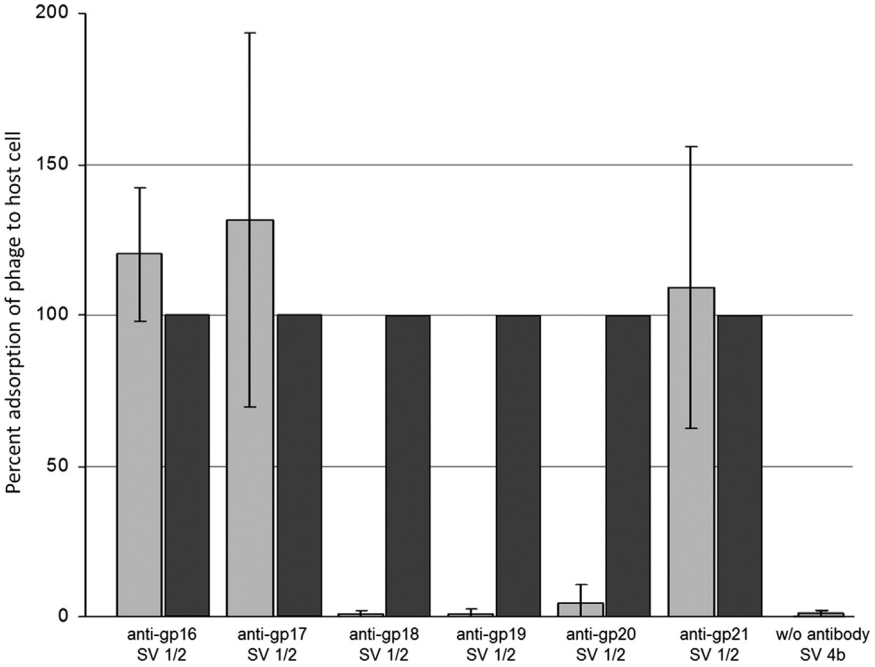

Fig. 3. Gp18, gp19, and gp20 play an important role in phage A118 attachment. Bacteriophage particles were pre-incubated with six different antibodies (α) directed against gp16 (Tmp) to gp21. Phages were then tested for their ability to attach to *Listeria* SV 1/2 host cells using pull down assays and determination of phage left in the supernatant. Plaque forming units (pfu) are given in % (light gray bars) and were normalized to the controls, which were A118 particles exposed to the corresponding pre-immune sera (dark gray bars) of the same animals, to exclude any variation introduced by individual antibody status of the different animals. Attachment of A118 on a serovar 4b strain was used as negative control.

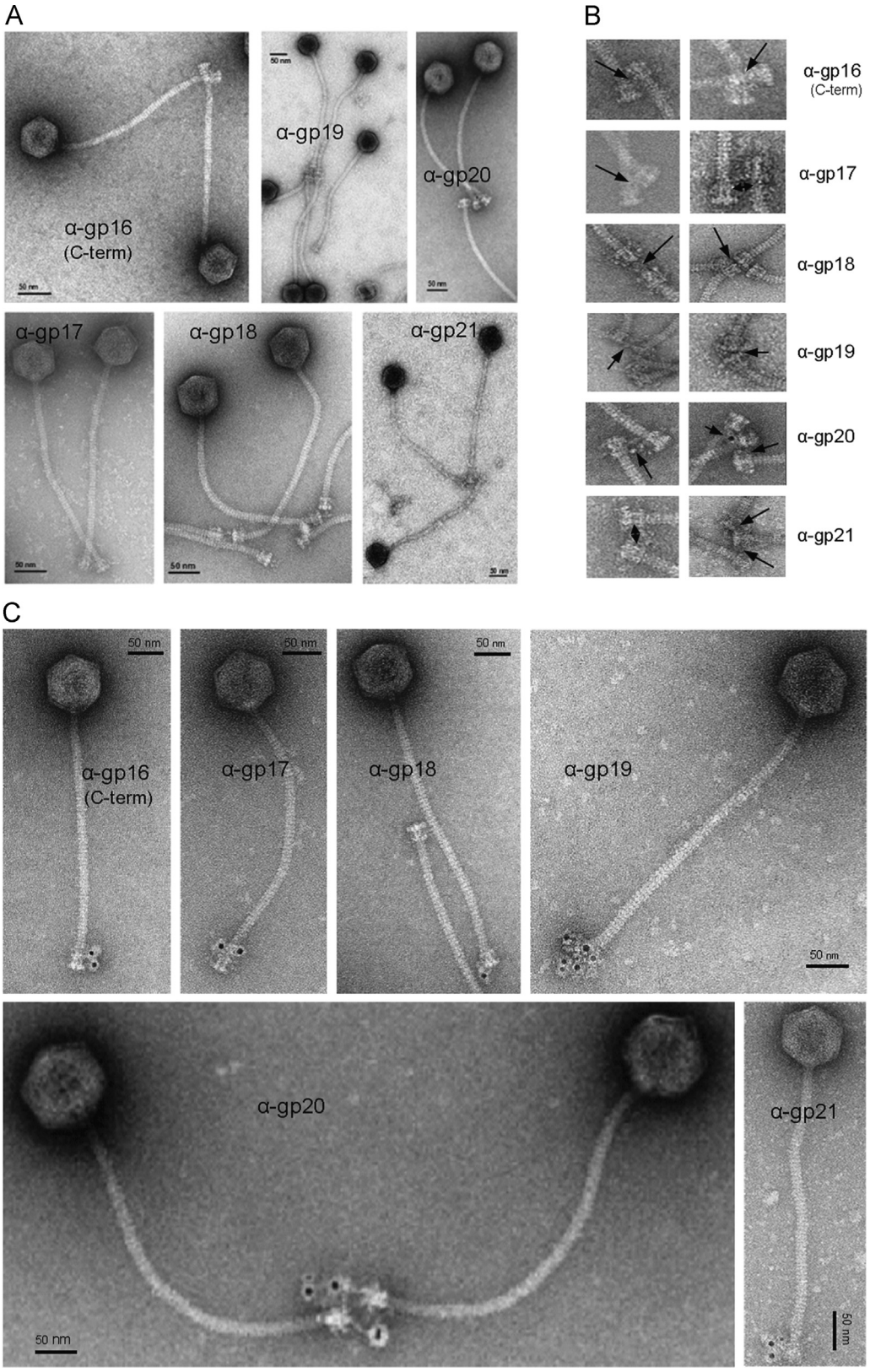

Fig. 4. EM-based identification of A118 baseplate proteins: (A) transmission electron microscopy of A118 particles crosslinked by pre-incubation with α-gp16 to α-gp21 antibodies. (B) Close-up of antibody-crosslinked baseplate proteins. Crosslinking sites are indicated by black arrows. (C) TEM images of immunogold-labeled A118 baseplate proteins. Phages were incubated with α-gp16, α-gp17, α-gp18, α-gp19, α-gp20 and α-gp21 and labeled with secondary antibodies conjugated to 5 nm gold particles. All scale bars correspond to 50 nm.

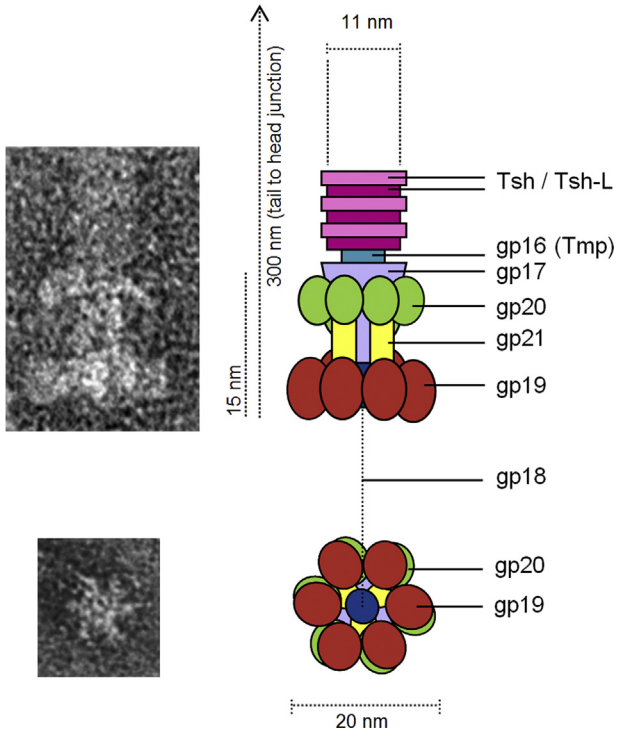

Fig. 5. Proposed model of the A118 baseplate. Results of the antibody-binding and crosslinking assays were summarized in a model of the phage tail tip, showing some anatomical features and approximate dimensions. The model (right) is aligned with TEM images (left). The central core is composed of the Dit-like protein gp17 (purple). The upper and a lower baseplate structures consist of gp20 (green) and gp19 (red) subunits, and are most likely arranged in a hexameric disk-like structure around the distal tail protein (gp17). Gp21 (yellow) provides a possible connection between both baseplate rings. The lower part of the baseplate is terminated by a central hub, created by the Tal-like gp18 (blue), which also serves as putative channel for DNA ejection and translocation (see text for explanation). The Tmp (cyan) is located inside the tail tube, but also accessible to antibodies at the interconnection of tail tube and tail tip, and provides a possible pathway for signal transduction. The tail tube is enclosed in a tail sheath (top of the structure), which is composed of Tsh/Tsh-L subunits (pink).

sequence homology, but also seem to feature different strategies for host recognition and phage attachment. *In silico* analysis revealed structural homologies of the putative baseplate proteins to known phage tail proteins, and allowed us to assign certain functions to the A118- and P35-encoded proteins. Among the large *Siphoviridae* group, two major clusters can be distinguished regarding baseplate organization and host attachment (Bebeacua et al., 2012). *Lactococcus* phages TP901-1, Tuc2009 or p2 exclusively interact with cell-wall saccharides and exhibit complex baseplates harboring multiple copies of RBPs for enhanced host affinity (Bebeacua et al., 2013; Ricagno et al., 2006; Spinelli et al., 2006a, 2006b; Tremblay et al., 2006). The other cluster comprises *E. coli* phage T5 and *Bacillus* phage SPP1, which feature a simpler tail-tip design and recognize saccharidic receptors in a first step, followed by irreversible binding to a proteinaceous host receptor (Baptista et al., 2008; Boulanger et al., 2008; Flayhan et al., 2012). A previous study proposed that both N-acetylglucosamine and rhamnose substituents in the WTA polymers serve as receptors for *Listeria* phage A118 (Wendlinger et al., 1996), while very recent work demonstrated that rhamnose alone is sufficient for host recognition and binding of A118 (Eugster et al., submitted for publication). Phage attachment is restricted to strains which feature rhamnose residues in the WTAs, and the recognition can effectively be inhibited by pre-incubation of the virus with rhamnose (Eugster and Loessner, 2012). We here show that A118 gp19 and gp20 acts as RBPs, and that rhamnose is required as host cell receptor. The presence of two separate phage RBPs indicates that A118 might use a TP901-1- or Tuc2009-like adsorption mechanism. It is conceivable that attachment of A118 occurs in a two-step process, in which the initial contact with the saccharide receptor is accomplished by one of the proteins, followed by enhanced binding via the secondary receptor, which triggers the subsequent events and is therefore irreversible. However, the precise mechanism and kinetics of this interaction remain to be determined.

The situation is somewhat different in phage P35, as only one RBP protein could be identified: Binding of GFP-tagged gp16 to a panel of 25 *Listeria* strains and mutants indicated that neither rhamnose nor N-acetylglucosamine alone are sufficient, but both are required for successful adsorption of the protein and the phage. The available evidence suggests that gp16 in fact represents the host specificity-determinant (Table 1). Interestingly, bioinformatics indicated that it has a homolog in *Listeria* phage P40, which seems taxonomically related to P35, but features a very different, almost complementary host range including strains of serovars 4, 5, and 6 (Dorscht et al., 2009b). Recent examination of this function showed that binding of P40 GFP-gp16 seems still limited to SV 1/2 cells only (unpublished data). This strongly suggests that other baseplate components should be involved in and responsible for the receptor recognition process in P40 and thereby determine host specificity.

Data obtained from antibody crosslinking and immunogold EM experiments were used to combine *in silico* findings with structural data, and allowed us to propose a topological model of the phage A118 tail and baseplate (Fig. 5). Based on the TEM images, the bulk of the A118 baseplate is composed of two ring-like structures. Gp19 could be localized at the lower ring of the baseplate, while gp20 forms part of the upper ring. The presence of such a double-disk structure has been previously proposed for *Lactococcus* phages TP901-1 and Tuc2009 (Sciara et al., 2008; Vegge et al., 2005). A118 gp20 features strong homologies to both baseplate proteins BppU and BppL of TP901-1. The lower baseplate of TP901-1 (BppL) and Tuc2009 (gp53) harbors the receptor binding function and an exchange of both proteins resulted in an altered host range of the chimeric phages (Vegge et al., 2006). Our findings indicate that the situation seems strikingly different in A118: both baseplate ring components exhibit a receptor binding function, and both proteins play a role in phage attachment. Phage adsorption can be completely inhibited by either α-gp19 or α-gp20 antisera (Fig. 3). Yet, the independent role of both elements awaits confirmation by other experimental approaches, including targeted mutagenesis of the respective phage genes.

The conserved order of Tmp (tape measure protein), Dit (distal tail protein), and Tal (tail associated lysozyme) encoding genes in several *Siphoviridae* genomes suggests a cross-talk between those proteins (Veesler et al., 2010). These three elements form an essential initiator complex for tail assembly. Phage propagation in the absence of Tmp, Dit or Tal resulted in tail-less phage particles (Vegge et al., 2005). This arrangement of Tmp, Dit and Tal is also conserved in A118 and P35. The Tmp and Dit homologs of P35 are directly followed by downstream gene specifying gp16, which harbors the receptor binding function. P35 gp14 and A118 gp16 represent the tape measure proteins (Tmp). The Tmp C-terminal domain is thought to possibly directly interact with the N-terminal domain of the TP901-1 central tail fiber (=Tal), perhaps providing a pathway for signal transduction (Veesler et al., 2012). An operon-based block cloning strategy including Dit/Bpp/BppL in TP901-1 as well as p2 ORFs 15/16/18 was used to demonstrate that Tal is not needed to obtain stable baseplates *in vitro*, suggesting a possible function in anchoring the baseplate to the phage tail, probably via interactions with the Tmp (Campanacci et al., 2010). The fact that the C-terminal domain of A118 Tmp is easily accessible to antibodies at the interconnection between tail and baseplate (Fig. 4C) suggests that it might also be

involved in tail to baseplate connection and signal transduction during infection.

A118 gp17 and P35 gp15 were identified as distal tail protein (Dit) homologs, which forms a central hub providing a possible anchor for tail tube, tail spike and possibly the baseplate, and assumes an essential role in adsorption apparatus assembly (Sciara et al., 2010; Veesler et al., 2010). TEM localization of A118 gp17 as shown here demonstrated that gp17 is accessible to antibodies from all sides (Fig. 4). It therefore likely forms the central core of the A118 baseplate, providing an attachment point for other baseplate proteins such as gp19 and gp20, which form the lower and upper baseplate disks (Fig. 5). Phage pull down assays confirmed that not only α-gp19 and α-gp20 can neutralize adsorption of A118, but also the α-gp18 antiserum (Fig. 3). A118 gp18 is homologous to baseplate protein gp44 of *Enterobacteriaceae* Myovirus Mu, which plays an essential role in phage assembly and generation of viable phages. It forms a hub-like structure with a central pore which was proposed to serve as a transit channel for genomic DNA (Kondou et al., 2005). Gp44 is a member of a group of gp27-like/Tal proteins, including T4 gp27 (Kanamaru et al., 2002) and p2 gp16 (Sciara et al., 2010), which feature structural similarities and a conserved tertiary structure (Veesler and Cambillau, 2011). Thus, A118 gp18, as well as P35 gp16, apparently represent the Tal proteins of these phages. In general, Tal proteins have been reported to play elemental roles in phage adsorption and infection as they are involved in cell wall puncturing and DNA release (Kenny et al., 2004; Kondou et al., 2005; Mc Grath et al., 2006). A central tail fiber composed of Tal trimers was found in lactococcal phages Tuc2009 and TP901-1, and is believed to possess lytic activity for localized degradation of the bacterial cell wall (Bebeacua et al., 2010; Kenny et al., 2004). TEM investigations (Fig. 4) yielded no evidence for a central tail spike at the A118 and P35 baseplates (Dorscht et al., 2009b). However, we could still locate gp18 in the center of the A118 lower baseplate. Previous work demonstrated that gp21 (Tal) of *Bacillus* phage SPP1 closely interacts with Dit and conformational changes from a “closed” to “open” position suggest a possible trigger leading to a cascade signaling pathway ending up in viral DNA ejection (Goulet et al., 2011; Plisson et al., 2007). The C-terminus of Tal is responsible for specific adsorption of SPP1 to the proteinaceous membrane receptor YueB (Baptista et al., 2008; Sao-Jose et al., 2004, 2006). Taken together, the precise role of the A118 Tal protein remains to be elucidated.

Material and methods

Bacterial strains and growth conditions

E. coli strain XL1-Blue MRF' (Stratagene, La Jolla, USA) was used for molecular cloning and protein production (Table S1). Cells were grown at 30 °C in LB medium (1% tryptone, 0.5% yeast extract, 1% NaCl, pH 7.4) under agitation and with the addition of Ampicillin (100 μg/ml) to maintain plasmid stability. All *Listeria* strains (Table S1) were grown in half-strength brain heart infusion (Biolife, Milan, Italy) at 30 °C with agitation. *Listeria* cell wall mutants had been constructed in the course of a previous project (Eugster et al., 2011; Eugster et al., submitted for publication).

Bacteriophage propagation

Phages and their characteristics are listed in Table S1. *Listeria ivanovii* strain WSLC 1001 (SV 1/2) was used for the propagation of *Listeria* phage A118, and *Listeria* strain Mack (SV 1/2) was used for propagation of phage P35. High titer phage stocks were obtained as described (Klumpp et al., 2008), followed by PEG precipitation (1 M NaCl, 10% PEG8000) (Yamamoto et al., 1970), and stepped CsCl-density gradient centrifugation (Loessner et al., 2000; Sambrook and Russell, 2001; Zink and Loessner, 1992). Phages stocks were stored at 4 °C in CsCl and dialyzed (Spectrapor membrane, MWCO 50,000) against SM Buffer (100 mM NaCl, 8 mM $MgSO_4$, 50 mM Tris–HCl, pH 7.5) immediately before use.

DNA techniques

DNA was amplified by PCR using Phusion polymerase (Finnzymes, Vantaa, Finland), following the manufacturer's instructions. Phage lysate or pure phage DNA was used as template. PCR primers were designed to contain overhanging restriction sites for cloning (Table S2). PCR products were digested with the appropriate restriction enzyme BamHI, SacI or SalI (Fermentas, Wohlen, Switzerland) and cloned into pQE-30 (Qiagen, Hilden, Germany), or its derivative pHGFP (Loessner et al., 2002), linearized with the same restriction enzymes. After transformation into electrocompetent cells, plasmids were isolated (GenElute Plasmid Miniprep Kit, Sigma-Aldrich, Buchs, Switzerland,) and the insert sequence was confirmed by Sanger sequencing (GATC Biotech, Konstanz, Germany).

Protein purification

Each protein of interest was produced in *E. coli* XL1-Blue after transformation with the appropriate recombinant plasmid, essentially as previously described (Schmelcher et al., 2010). Briefly, protein production was induced in modified LB media (15 g/L tryptose, 8 g/L yeast extract 5 g/L NaCl) with 100 mM IPTG (Sigma-Aldrich) added as inducer once an $OD_{600\ nm}$ of 0.5 was reached. Protein expression was induced for 4 h at 15 °C and cells were harvested by centrifugation and disrupted by passage through a Stansted SPCH-10 pressure homogenizer (Stansted Fluid Power Ltd, Harlow, UK) at 100 MPa pressure, then centrifuged and filtered. Proteins were purified by immobilized metal affinity chromatography (IMAC) by using MicroBiospin columns (Bio-Rad, Cressier, Switzerland) packed with Ni-NTA Superflow resin (Qiagen). Buffer B (500 mM NaCl, 50 mM Na_2HPO_4, 250 mM imidazole, 0.1% Tween 20 [pH 8.0]) was used for the elution of His-tagged proteins (Schmelcher et al., 2010).

Antibody generation

Polyclonal rabbit-antibodies were generated at the Institute of Laboratory Animal Science, University of Zurich, Switzerland, in accordance with all animal welfare regulations. A standard 10-week immunization protocol was used. The protocols included pre-immunization at day 0, an initial injection at day 1 (together with Freund's Complete Adjuvant, Sigma), and boost injections at days 28 and 56. A total of 250 μg protein was used for the injections, with 500 μl volume per s.c. injection, together with Freund's Incomplete Adjuvant (Sigma-Aldrich, 50 μl per injection site). Sera obtained from the bleed 2 weeks after the final boost were ProteinA purified (ProteinA-antibody purification Kit, Sigma) to obtain the IgG fraction to be used for further experiments.

Cell wall decoration assays

Binding assays using purified GFP-RBP-fusion proteins were carried out in order to assess cell wall binding by the recombinant protein (Figs. 1 and 2). The assay was performed as described earlier (Loessner et al., 2002). Purified GFP-RBP-fusion proteins were centrifuged for 1 h with 30,000*g* at 4 °C to remove potential protein aggregations. 0.5 ml of exponentially growing bacterial cells were centrifuged and resuspended in 120 μl of SM buffer and incubated together with 5 μg of GFP-RBP for 1 h at room temperature. Cells were washed twice with SM buffer and binding to the bacterial cells was checked by confocal fluorescence microscopy (Leica TCS SPE confocal microscope, Leica Microsystems GmbH, Wetzlar, Germany).

Phage host range

Host range analysis was performed as described elsewhere by double agar overlay assays and spot-on-the-lawn assays (Kropinski et al., 2009; Loessner and Busse, 1990). A total of 26 *Listeria* strains were tested, including six cell wall mutants (Supplementary Table S1).

Phage adsorption pull down assay

Pull-down assays were performed to evaluate the adsorption characteristics of phage to host cells. 100 μl of phage suspensions (10^7 pfu/ml) were used, some were pre-incubated with 5 μl of antiserum for 1 h at room temperature (Fig. 3). Following, samples were incubated for 10 min with 0.5 ml of an overnight culture of the respective *Listeria* strains grown in half-strength BHI media. Samples with pre-immune sera incubation served as controls for antibody inhibition assays (Fig. 3). Cells were centrifuged for 2 min with 12,000*g* and the pellet was washed twice in PBST (pH 8.0). After dilution, double agar overlay assays were performed, mixing host cells with either supernatant or pellet. Following an overnight incubation at 30 °C, plaques were enumerated. All counts were normalized to 100% (propagation host strain in standard pull down assays (Figs. S2 and S3); and pre-immune serum from same rabbit in antibody pre-incubation pull down experiments (Fig. 3)), and values above 25% were considered as positive for the composition of Table 1.

Transmission electron microscopy

CsCl-purified phage particles (10 μl of 10^{12} pfu/ml) were mixed with 990 μl of TBT buffer (20 mM Tris, 50 mM NaCl, 10 mM $MgCl_2$), and incubated with 10 μl antiserum. After overnight incubation, the sample was purified twice by passage of the mixture through Sephacryl S-400 (Promega, Dübendorf, Switzerland) gravity-flow columns. Phages present in the flow-through were then either directly prepared for TEM, or further incubated with 5 μl of the secondary 5 nm gold conjugate goat anti-rabbit IgG antibody (5 nm GAR, British Biocell, Cardiff, UK). Again, phages were passed through Sephacryl S-400 columns after incubation to remove unbound antibodies. Negative stains were prepared with 2% uranyl acetate or 2% ammoniummolybdate solution, and samples were adsorbed on carbon-coated G400 Hex-C3 grids (Science Services, Munich, Germany) (Steven et al., 1988). The samples were observed in a Tecnai G2 Spirit microscope at 120 kV, equipped with an EAGLE CCD camera (FEI, Hillsboro, OR, USA).

Bioinformatics

Nucleotide and amino acid sequence analysis and interpretation were performed using CLC Genomics Workbench (Version 7, CLC Bio, Aarhus, Denmark). BLASTn, BLASTp and LALIGN algorithms were used for pairwise sequence alignments (Altschul et al., 1990, 1997; Pearson et al., 1997). HHpred was used to determine structural similarities and sequence homologs (Soding, 2005).

Appendix A. Supporting information

Supplementary data associated with this article can be found in the online version at: http://dx.doi.org/10.1016/j.virol.2014.12.035.

References

Altschul, S.F., Gish, W., Miller, W., Myers, E.W., Lipman, D.J., 1990. Basic local alignment search tool. J. Mol. Biol. 215, 403–410.

Altschul, S.F., Madden, T.L., Schaffer, A.A., Zhang, J., Zhang, Z., Miller, W., Lipman, D.J., 1997. Gapped BLAST and PSI-BLAST: a new generation of protein database search programs. Nucleic Acids Res. 25, 3389–3402.

Baptista, C., Santos, M.A., Sao-Jose, C., 2008. Phage SPP1 reversible adsorption to *Bacillus subtilis* cell wall teichoic acids accelerates virus recognition of membrane receptor YueB. J. Bacteriol. 190, 4989–4996.

Barbirz, S., Muller, J.J., Uetrecht, C., Clark, A.J., Heinemann, U., Seckler, R., 2008. Crystal structure of *Escherichia coli* phage HK620 tailspike: podoviral tailspike endoglycosidase modules are evolutionarily related. Mol. Microbiol. 69, 303–316.

Bebeacua, C., Bron, P., Lai, L., Vegge, C.S., Brondsted, L., Spinelli, S., Campanacci, V., Veesler, D., van Heel, M., Cambillau, C., 2010. Structure and molecular assignment of lactococcal phage TP901-1 baseplate. J. Biol. Chem. 285, 39079–39086.

Bebeacua, C., Lai, L., Vegge, C.S., Brondsted, L., van Heel, M., Veesler, D., Cambillau, C., 2012. Visualizing a complete *Siphoviridae* by single-particle electron microscopy: the structure of lactococcal phage TP901-1. J. Virol..

Bebeacua, C., Tremblay, D., Farenc, C., Chapot-Chartier, M.P., Sadovskaya, I., van Heel, M., Veesler, D., Moineau, S., Cambillau, C., 2013. Structure, adsorption to host, and infection mechanism of virulent lactococcal phage p2. J. Virol. 87, 12302–12312.

Bertsch, D., Rau, J., Eugster, M.R., Haug, M.C., Lawson, P.A., Lacroix, C., Meile, L., 2013. *Listeria fleischmannii* sp. nov., isolated from cheese. Int. J. Syst. Evol. Microbiol. 63, 526–532.

Boulanger, P., Jacquot, P., Plancon, L., Chami, M., Engel, A., Parquet, C., Herbeuval, C., Letellier, L., 2008. Phage T5 straight tail fiber is a multifunctional protein acting as a tape measure and carrying fusogenic and muralytic activities. J. Biol. Chem. 283, 13556–13564.

Campanacci, V., Veesler, D., Lichiere, J., Blangy, S., Sciara, G., Moineau, S., van Sinderen, D., Bron, P., Cambillau, C., 2010. Solution and electron microscopy characterization of lactococcal phage baseplates expressed in *Escherichia coli*. J. Struct. Biol. 172, 75–84.

Carlton, R.M., Noordman, W.H., Biswas, B., De Meester, E.D., Loessner, M.J., 2005. Bacteriophage P100 for control of *Listeria monocytogenes* in foods: genome sequence, bioinformatic analyses, oral toxicity study, and application. Regul. Toxicol. Pharmacol. 43, 301–312.

Chatterjee, S., Rothenberg, E., 2012. Interaction of bacteriophage l with its *E. coli* receptor, LamB. Viruses 4, 3162–3178.

De Haard, H.J., Bezemer, S., Ledeboer, A.M., Muller, W.H., Boender, P.J., Moineau, S., Coppelmans, M.C., Verkleij, A.J., Frenken, L.G., Verrips, C.T., 2005. Llama antibodies against a lactococcal protein located at the tip of the phage tail prevent phage infection. J. Bacteriol. 187, 4531–4541.

Dorscht, J., Klumpp, J., Bielmann, R., Schmelcher, M., Born, Y., Zimmer, M., Calendar, R., Loessner, M., 2009a. Comparative genome analysis of *Listeria* bacteriophages reveals extensive mosaicism, programmed translational frameshifting, and a novel prophage insertion site. J. Bacteriol. 191, 7206–7215.

Dorscht, J., Klumpp, J., Bielmann, R., Schmelcher, M., Born, Y., Zimmer, M., Calendar, R., Loessner, M.J., 2009b. Comparative genome analysis of *Listeria* bacteriophages reveals extensive mosaicism, programmed translational frameshifting, and a novel prophage insertion site. J. Bacteriol. 191, 7206–7215.

Duplessis, M., Moineau, S., 2001. Identification of a genetic determinant responsible for host specificity in *Streptococcus thermophilus* bacteriophages. Mol. Microbiol. 41, 325–336.

Dupont, K., Vogensen, F.K., Neve, H., Bresciani, J., Josephsen, J., 2004. Identification of the receptor-binding protein in 936-species lactococcal bacteriophages. Appl. Environ. Microbiol. 70, 5818–5824.

Eugster, M.R., Haug, M.C., Huwiler, S.G., Loessner, M.J., 2011. The cell wall binding domain of Listeria bacteriophage endolysin PlyP35 recognizes terminal GlcNAc residues in cell wall teichoic acid. Mol. Microbiol. 81, 1419–1432.

Eugster, M.R., Loessner, M.J., 2012. Wall teichoic acids restrict access of bacteriophage endolysin Ply118, Ply511, and PlyP40 cell wall binding domains to the *Listeria* monocytogenes peptidoglycan. J. Bacteriol. 194, 6498–6506.

Eugster, M.R., Morax, L.S., Huels, V.J., Huwiler, S.G., Leclercq, A., Lecuit, M., Loessner, M.J. Bacteriophage predation promotes serovar diversification in *Listeria monocytogenes* (submitted for publication).

Farber, J.M., Peterkin, P.I., 1991. *Listeria monocytogenes*, a food-borne pathogen. Microbiol. Rev. 55, 476–511.

Fiedler, F., 1988. Biochemistry of the cell surface of *Listeria* strains: a locating general view. Infection 16 (Suppl. 2), S92–S97.

Flayhan, A., Wien, F., Paternostre, M., Boulanger, P., Breyton, C., 2012. New insights into pb5, the receptor binding protein of bacteriophage T5, and its interaction with its *Escherichia coli* receptor FhuA. Biochimie 94, 1982–1989.

Goulet, A., Lai-Kee-Him, J., Veesler, D., Auzat, I., Robin, G., Shepherd, D.A., Ashcroft, A.E., Richard, E., Lichiere, J., Tavares, P., Cambillau, C., Bron, P., 2011. The opening of the SPP1 bacteriophage tail, a prevalent mechanism in Gram-positive-infecting siphophages. J. Biol. Chem. 286, 25397–25405.

Graves, L.M., Helsel, L.O., Steigerwalt, A.G., Morey, R.E., Daneshvar, M.I., Roof, S.E., Orsi, R.H., Fortes, E.D., Milillo, S.R., den Bakker, H.C., Wiedmann, M., Swaminathan, B., Sauders, B.D., 2010. *Listeria marthii* sp. nov., isolated from the natural environment, Finger Lakes National Forest. Int. J. Syst. Evol. Microbiol. 60, 1280–1288.

Guo, S., Shu, D., Simon, M.N., Guo, P., 2003. Gene cloning, purification, and stoichiometry quantification of phi29 anti-receptor gp12 with potential use as special ligand for gene delivery. Gene 315, 145–152.

Habann, M., Leiman, P.G., Vandersteegen, K., Van den Bossche, A., Lavigne, R., Shneider, M.M., Bielmann, R., Eugster, M.R., Loessner, M.J., Klumpp, J., 2014. *Listeria* phage A511, a model for the contractile tail machineries of SPO1-related bacteriophages. Mol. Microbiol. 92, 84–99.

Hagens, S., De Wouters, T., Vollenweider, P., Loessner, M.J., 2011. Reporter bacteriophage A511::celB transduces a hyperthermostable glycosidase from *Pyrococcus furiosus* for rapid and simple detection of viable *Listeria* cells. Bacteriophage 1, 143–151.

Jakutyte, L., Lurz, R., Baptista, C., Carballido-Lopez, R., Sao-Jose, C., Tavares, P., Daugelavicius, R., 2012. First steps of bacteriophage SPP1 entry into *Bacillus subtilis*. Virology 422, 425–434.
Kanamaru, S., Leiman, P.G., Kostyuchenko, V.A., Chipman, P.R., Mesyanzhinov, V.V., Arisaka, F., Rossmann, M.G., 2002. Structure of the cell-puncturing device of bacteriophage T4. Nature 415, 553–557.
Katsura, I., 1987. Determination of bacteriophage lambda tail length by a protein ruler. Nature 327, 73–75.
Kenny, J.G., McGrath, S., Fitzgerald, G.F., van Sinderen, D., 2004. Bacteriophage Tuc2009 encodes a tail-associated cell wall-degrading activity. J. Bacteriol. 186, 3480–3491.
Killmann, H., Videnov, G., Jung, G., Schwarz, H., Braun, V., 1995. Identification of receptor binding sites by competitive peptide mapping: phages T1, T5, and phi 80 and colicin M bind to the gating loop of FhuA. J. Bacteriol. 177, 694–698.
Klumpp, J., Dorscht, J., Lurz, R., Bielmann, R., Wieland, M., Zimmer, M., Calendar, R., Loessner, M.J., 2008. The terminally redundant, nonpermuted genome of *Listeria* bacteriophage A511: a model for the SPO1-like myoviruses of Gram-positive bacteria. J. Bacteriol. 190, 5753–5765.
Kondou, Y., Kitazawa, D., Takeda, S., Tsuchiya, Y., Yamashita, E., Mizuguchi, M., Kawano, K., Tsukihara, T., 2005. Structure of the central hub of bacteriophage Mu baseplate determined by X-ray crystallography of gp44. J. Mol. Biol. 352, 976–985.
Kropinski, A.M., Mazzocco, A., Waddell, T.E., Lingohr, E., Johnson, R.P., 2009. Enumeration of bacteriophages by double agar overlay plaque assay. Methods Mol. Biol. 501, 69–76.
Lang Halter, E., Neuhaus, K., Scherer, S., 2013. *Listeria weihenstephanensis* sp. nov., isolated from the water plant *Lemna trisulca* taken from a freshwater pond. Int. J. Syst. Evol. Microbiol. 63, 641–647.
Leclercq, A., Clermont, D., Bizet, C., Grimont, P.A., Le Fleche-Mateos, A., Roche, S.M., Buchrieser, C., Cadet-Daniel, V., Le Monnier, A., Lecuit, M., Allerberger, F., 2010. *Listeria rocourtiae* sp. nov. Int. J. Syst. Evol. Microbiol. 60, 2210–2214.
Leiman, P.G., Arisaka, F., van Raaij, M.J., Kostyuchenko, V.A., Aksyuk, A.A., Kanamaru, S., Rossmann, M.G., 2010. Morphogenesis of the T4 tail and tail fibers. Virol. J. 7, 355.
Loessner, M.J., 1991. Improved procedure for bacteriophage typing of *Listeria* strains and evaluation of new phages. Appl. Environ. Microbiol. 57, 882–884.
Loessner, M.J., Busse, M., 1990. Bacteriophage typing of *Listeria* species. Appl. Environ. Microbiol. 56, 1912–1918.
Loessner, M.J., Inman, R.B., Lauer, P., Calendar, R., 2000. Complete nucleotide sequence, molecular analysis and genome structure of bacteriophage A118 of *Listeria monocytogenes*: implications for phage evolution. Mol. Microbiol. 35, 324–340.
Loessner, M.J., Kramer, K., Ebel, F., Scherer, S., 2002. C-terminal domains of *Listeria monocytogenes* bacteriophage murein hydrolases determine specific recognition and high-affinity binding to bacterial cell wall carbohydrates. Mol. Microbiol. 44, 335–349.
Loessner, M.J., Rees, C.E., Stewart, G.S., Scherer, S., 1996. Construction of luciferase reporter bacteriophage A511::luxAB for rapid and sensitive detection of viable *Listeria* cells. Appl. Environ. Microbiol. 62, 1133–1140.
Loessner, M.J., Wendlinger, G., Scherer, S., 1995. Heterogeneous endolysins in *Listeria* monocytogenes bacteriophages: a new class of enzymes and evidence for conserved holin genes within the siphoviral lysis cassettes. Mol. Microbiol. 16, 1231–1241.
Marti, R., Zurfluh, K., Hagens, S., Pianezzi, J., Klumpp, J., Loessner, M.J., 2013. Long tail fibers of the novel broad host range T-even bacteriophage S16 specifically recognize *Salmonella* OmpC. Mol. Microbiol. 87, 818–834.
Mc Grath, S., Neve, H., Seegers, J.F., Eijlander, R., Vegge, C.S., Brondsted, L., Heller, K.J., Fitzgerald, G.F., Vogensen, F.K., van Sinderen, D., 2006. Anatomy of a lactococcal phage tail. J. Bacteriol. 188, 3972–3982.
Muller, J.J., Barbirz, S., Heinle, K., Freiberg, A., Seckler, R., Heinemann, U., 2008. An intersubunit active site between supercoiled parallel beta helices in the trimeric tailspike endorhamnosidase of *Shigella flexneri* Phage Sf6. Structure 16, 766–775.
Pearson, W.R., Wood, T., Zhang, Z., Miller, W., 1997. Comparison of DNA sequences with protein sequences. Genomics 46, 24–36.
Plisson, C., White, H.E., Auzat, I., Zafarani, A., Sao-Jose, C., Lhuillier, S., Tavares, P., Orlova, E.V., 2007. Structure of bacteriophage SPP1 tail reveals trigger for DNA ejection. EMBO J. 26, 3720–3728.
Ricagno, S., Campanacci, V., Blangy, S., Spinelli, S., Tremblay, D., Moineau, S., Tegoni, M., Cambillau, C., 2006. Crystal structure of the receptor-binding protein head domain from *Lactococcus lactis* phage bIL170. J. Virol. 80, 9331–9335.
Rossman, M.G., Yap, M.L., 2014. Structure and function of bacteriophage T4. Future Med. 9, 1319–1327.
Sambrook, J., Russell, D.W., 2001. Molecular Cloning – A Laboratory Manual, 3rd ed. Cold Spring Harbor Laboratory Press, New York.
Sao-Jose, C., Baptista, C., Santos, M.A., 2004. *Bacillus subtilis* operon encoding a membrane receptor for bacteriophage SPP1. J. Bacteriol. 186, 8337–8346.
Sao-Jose, C., Lhuillier, S., Lurz, R., Melki, R., Lepault, J., Santos, M.A., Tavares, P., 2006. The ectodomain of the viral receptor YueB forms a fiber that triggers ejection of bacteriophage SPP1 DNA. J. Biol. Chem. 281, 11464–11470.
Schmelcher, M., Shabarova, T., Eugster, M.R., Eichenseher, F., Tchang, V.S., Banz, M., Loessner, M.J., 2010. Rapid multiplex detection and differentiation of *Listeria* cells by use of fluorescent phage endolysin cell wall binding domains. Appl. Environ. Microbiol. 76, 5745–5756.
Sciara, G., Bebeacua, C., Bron, P., Tremblay, D., Ortiz-Lombardia, M., Lichiere, J., van Heel, M., Campanacci, V., Moineau, S., Cambillau, C., 2010. Structure of lactococcal phage p2 baseplate and its mechanism of activation. Proc. Natl. Acad. Sci. USA 107, 6852–6857.
Sciara, G., Blangy, S., Siponen, M., Mc Grath, S., van Sinderen, D., Tegoni, M., Cambillau, C., Campanacci, V., 2008. A topological model of the baseplate of lactococcal phage Tuc2009. J. Biol. Chem. 283, 2716–2723.
Siponen, M., Sciara, G., Villion, M., Spinelli, S., Lichiere, J., Cambillau, C., Moineau, S., Campanacci, V., 2009. Crystal structure of ORF12 from *Lactococcus lactis* phage p2 identifies a tape measure protein chaperone. J. Bacteriol. 191, 728–734.
Soding, J., 2005. Protein homology detection by HMM–HMM comparison. Bioinformatics 21, 951–960.
Spinelli, S., Campanacci, V., Blangy, S., Moineau, S., Tegoni, M., Cambillau, C., 2006a. Modular structure of the receptor binding proteins of *Lactococcus lactis* phages. The RBP structure of the temperate phage TP901-1. J. Biol. Chem. 281, 14256–14262.
Spinelli, S., Desmyter, A., Verrips, C.T., De Haard, H.J., Moineau, S., Cambillau, C., 2006b. Lactococcal bacteriophage p2 receptor-binding protein structure suggests a common ancestor gene with bacterial and mammalian viruses. Nat. Struct. Mol. Biol. 13, 85–89.
Spinelli, S., Veesler, D., Bebeacua, C., Cambillau, C., 2014. Structures and host-adhesion mechanisms of lactococcal siphophages. Front. Microbiol. 5, 3.
Steven, A.C., Trus, B.L., Maizel, J.V., Unser, M., Parry, D.A., Wall, J.S., Hainfeld, J.F., Studier, F.W., 1988. Molecular substructure of a viral receptor-recognition protein. The gp17 tail-fiber of bacteriophage T7. J. Mol. Biol. 200, 351–365.
Stuer-Lauridsen, B., Janzen, T., Schnabl, J., Johansen, E., 2003. Identification of the host determinant of two prolate-headed phages infecting *Lactococcus lactis*. Virology 309, 10–17.
Tremblay, D.M., Tegoni, M., Spinelli, S., Campanacci, V., Blangy, S., Huyghe, C., Desmyter, A., Labrie, S., Moineau, S., Cambillau, C., 2006. Receptor-binding protein of *Lactococcus lactis* phages: identification and characterization of the saccharide receptor-binding site. J. Bacteriol. 188, 2400–2410.
Uchikawa, K., Sekikawa, I., Azuma, I., 1986. Structural studies on teichoic acids in cell walls of several serotypes of *Listeria monocytogenes*. J. Biochem. 99, 315–327.
Vazquez-Boland, J.A., Kuhn, M., Berche, P., Chakraborty, T., Dominguez-Bernal, G., Goebel, W., Gonzalez-Zorn, B., Wehland, J., Kreft, J., 2001. *Listeria* pathogenesis and molecular virulence determinants. Clin. Microbiol. Rev. 14, 584–640.
Veesler, D., Cambillau, C., 2011. A common evolutionary origin for tailed-bacteriophage functional modules and bacterial machineries. Microbiol. Mol. Biol. Rev. 75, 423–433.
Veesler, D., Robin, G., Lichiere, J., Auzat, I., Tavares, P., Bron, P., Campanacci, V., Cambillau, C., 2010. Crystal structure of bacteriophage SPP1 distal tail protein (gp19.1): a baseplate hub paradigm in Gram-positive infecting phages. J. Biol. Chem. 285, 36666–36673.
Veesler, D., Spinelli, S., Mahony, J., Lichiere, J., Blangy, S., Bricogne, G., Legrand, P., Ortiz-Lombardia, M., Campanacci, V., van Sinderen, D., Cambillau, C., 2012. Structure of the phage TP901-1 1.8 MDa baseplate suggests an alternative host adhesion mechanism. Proc. Natl. Acad. Sci. USA 109, 8954–8958.
Vegge, C.S., Brondsted, L., Neve, H., Mc Grath, S., van Sinderen, D., Vogensen, F.K., 2005. Structural characterization and assembly of the distal tail structure of the temperate lactococcal bacteriophage TP901-1. J. Bacteriol. 187, 4187–4197.
Vegge, C.S., Vogensen, F.K., Mc Grath, S., Neve, H., van Sinderen, D., Brondsted, L., 2006. Identification of the lower baseplate protein as the antireceptor of the temperate lactococcal bacteriophages TP901-1 and Tuc2009. J. Bacteriol. 188, 55–63.
Wang, J., Hofnung, M., Charbit, A., 2000. The C-terminal portion of the tail fiber protein of bacteriophage lambda is responsible for binding to LamB, its receptor at the surface of *Escherichia coli* K-12. J. Bacteriol. 182, 508–512.
Wendlinger, G., Loessner, M.J., Scherer, S., 1996. Bacteriophage receptors on *Listeria monocytogenes* cells are the N-acetylglucosamine and rhamnose substituents of teichoic acids or the peptidoglycan itself. Microbiology 142 (Part 4), 985–992.
Werts, C., Michel, V., Hofnung, M., Charbit, A., 1994. Adsorption of bacteriophage lambda on the LamB protein of *Escherichia coli* K-12: point mutations in gene J of lambda responsible for extended host range. J. Bacteriol. 176, 941–947.
Yamamoto, K.R., Alberts, B.M., Benzinger, R., Lawhorne, L., Treiber, G., 1970. Rapid bacteriophage sedimentation in the presence of polyethylene glycol and its application to large-scale virus purification. Virology 40, 734–744.
Zink, R., Loessner, M.J., 1992. Classification of virulent and temperate bacteriophages of *Listeria* spp. on the basis of morphology and protein analysis. Appl. Environ. Microbiol. 58, 296–302.